Geomechanics and Engineering, *Vol. 16, No. 1 (2018) 97-104*
DOI: https://doi.org/10.12989/gae.2018.16.1.097

Study on deformation law of surrounding rock of super long and deep buried sandstone tunnel

Lujun Ding*[1] and Yuhong Liu[2a]

[1]College of Water Resource and Hydropower, Sichuan University, Chengdu, 610065, China
[2]Sichuan College of Architectural Technology, Deyang, 618000, China

(Received December 26, 2017, Revised March 9, 2018, Accepted April 7, 2018)

Abstract. The finite difference software Flac3D is used to study the influence of tunnel burial depth, tunnel diameter and lateral pressure coefficient of original rock stress on the stress and deformation of tunnel surrounding rock under sandstone condition. The results show that the maximum shear stress, the radius of the plastic zone and the maximum displacement in the surrounding rock increase with the increase of the diameter of the tunnel. When the lateral pressure coefficient is 1, it is most favorable for surrounding rock and lining structure, with the increase or decrease of lateral pressure coefficient, the maximum principal stress, surrounding displacement and plastic zone range of surrounding rock and lining show a sharp increase trend, the plastic zone on the lining increases with the increase of buried depth.

Keywords: water conveyance tunnel; deformation of surrounding rock; numerical simulation; the lateral pressure coefficient; buried depth

1. Introduction

Water diversion projects in large and trans basin mountainous areas often involve many underground water conveyance tunnels, especially when the watershed elevation is much higher than the water pass bed elevation, cut across the watershed of the deep underground water tunnel often become the realization of water diversion to an effective and economical way. The deformation and stability of surrounding rock of buried water conveyance tunnel is one of the main problems that need to be studied and considered in the field of water conservancy and hydropower engineering and railway, highway tunnel engineering and mining engineering.

Due to the numerous factors affecting the stability of surrounding rock and the stability of lining structure, and the uncertainty of the physical and mechanical properties of the surrounding rock and the irregularity of the original rock stress field, it is very difficult to solve the theoretical analysis solution of the stability of the surrounding rock of the water conveyance tunnel. With the rapid development of computer technology, the deformation law of underground engineering can be simulated by numerical method, and the deformation of surrounding rock, the redistribution of geostress field and the scope of plastic zone are analyzed, so as to evaluate the stability of surrounding rock.

Xie (2004) have described the variation rule of the damage variable and the coupled variable-damage energy dissipation rate by the damage evolution equation. Alireza (2014) made a numerical modeling of the nailed walls with a view to assess the stability. Alireza observed a nailing system with a excavation depth of 8 meters by using the three constitutive behavioral methods. Ali (2018) estimated geomechanical parameters such as rock quality designation and uniaxial compressive strength of Azad dam by ordinary kriging as a geostatistical method, and presented specified distribution maps for each parameter. Liu (2015) studied the deformation process of tunnel surrounding rock and lining by numerical simulation and field measurement. Liu (2015) presented a gradient-dependent plastic model that considers the strain-softening behavior, according to the test results of the soil strength, which reduces from peak to residual strength, the Mohr-Coulomb criterion that considers strain-softening under gradient plastic theory is deduced.

Yoo (2016) used the 3DFE model, a parametric study was conducted on a number of tunneling cases with emphasis on the spatial characteristics of the weak zone such as the strike and dip angle, and on the initial stress state. Małkowski (2015) analyzed the area of influence of a reasonable numerical model on surrounding rock failure on roadway, and compared it with field test by considering the elastic and elasto-plastic models. Su (2016) considering landslides, distortion of steel arch and frequent arch changing occur easily for large cross section tunnels of carbide argillite in the course of construction, Selected multiple monitor sections near the entrances and exits of Xiaopanling tunnels for the field test.

Sheng (2017) describes a case study of the failure mechanisms and stability control technology of deep roadway with soft rock mass in Xin’an coal mine in Gansu Province, China. Rock mass properties around the roadway are evaluated using geological strength index based on the field data and the mechanical properties of intact rock specimens. Some scholars (Zhu 2013, Siddiquee 2013) have

*Corresponding author, Assistant Professor
E-mail: mddh966@126.com
[a]Research Assistant

ISSN: 2005-307X (Print), 2092-6219 (Online)

studied elasto-viscoplastic model and nonlinear model for soft rock around tunnels. Yu (2017) analyzed on deformation and failure zone distribution laws of surrounding rock in deep-buried soft rock tunnel. Liu (2016) describes the application of the method in detail, and evaluates the construction effect from three aspects, including the ability to control surrounding rock deformation, construction schedule and risk control. There are three indicators for the evaluation of deformation and stability of surrounding rock, including vault settlement, steel arch force and fiberglass anchor. Li (2014) simulated the rectangular tunnel deformation and failure through the cvisc viscoelastic plastic model of $FLAC^{3D}$. Chen (2016) proposed a new reinforcement algorithms in discontinuous deformation analysis for rock failure.

This paper analyzed the surface friction and axial force distribution law of the bolt body by the coordination function principle between surrounding rock and bolt and the maximum axial force value of bolt neutral point was derived according to the static equilibrium condition. On this basis, the formulas about the radius of plastic zone and loose zone after the surrounding rock deformation ceased were proposed. Finally, it determined theoretically loose zone and plastic zone range of Liutongzhai tunnel surrounding rock, which provided important technical support for optimization of surrounding rock support scheme as well as parameters. Su Yonghua by tracking the disintegration of the granules of varying levels of process debris found that soft rock swelling collapse process is a multifractal process, when the collapse to a certain extent, the level of the debris particle disintegration will no longer change, soft rock swelling is stopped, the fractal dimension of the slaking substance reaches a critical value no longer change. Nikadat and Marji (2016) evaluated the effects of two basic geometric factors influencing tunnel behavior in a jointed rock mass; joints spacing and joints orientation.

In west of South to North Water Diversion Project surrounding rock tunnel sandstone under the condition as the research object, numerical simulation using finite difference program $Flac^{3D}$ sandstone section of deep buried tunnel pre excavation, analysis of tunnel diameter, buried depth, lateral pressure coefficient of the change of tunnel surrounding rock and lining structure, the influence of stress displacement.

2. Engineering situation

2.1 The main deformation parameters of the structural plane

When studying the deformation parameters of the structural plane, the structural plane is generalized to the interface layer with a certain thickness. Because the sandstone level of the surrounding rock of the west line project belongs to micro weathering or weak weathering, and the wall rock is hard. According to the literature, it is calculated that the tangential stiffness of the structural plane is 4.70e10 MPa/m, and the normal stiffness of the structural plane is 1.59e10 MPa/m.

Table 1 Main physical and mechanical parameters of rock

Rock stratum	Deformation modulus /GPa	Poisson ratio	Cohesive force /MPa	Internal friction angle /°	Bulk density /KN·m^3	Tensile strength /MPa
Sandstone	9.9	0.22	2.0	46	27	10.0

Table 2 Lining structure parameter table

Elastic modulus /GPa	Poisson ratio	Bulk density /kN/m^3	Cohesive force /MPa	Internal friction angle /°	Compressive strength /MPa
34.5	0.17	25	10	50	50

2.2 Physical and mechanical parameters

There is a great difference between the physical and mechanical parameters of rock and the physical and mechanical parameters of the rock mass in the field. Therefore, the physical and mechanical parameters of the rock mass measured in the laboratory will be modified by the method in reference (Ma 2015, Liu 2015) to get the ideal value which is closer to the engineering rock mass. After reduction, the main physical and mechanical parameters of rock needed for analysis and calculation can be obtained, as shown in Table 1.

The lining material is concrete (C50), and the thickness of the lining is 0.5 m. It is simplified as the analysis of the homogeneous ring. The main parameters are shown in Table 2.

2.3 Elastoplastic constitutive model

According to the deformation of surrounding rock and the material properties of surrounding rock, the elasto-plastic constitutive M-C model is adopted for surrounding rock. The large strain deformation model is adopted for lining, and the failure criterion is based on the M-C strength criterion.

3. Numerical simulation of the stability of tunnel surrounding rock and lining under sandstone conditions

3.1 Calculation model and mesh generation

The numerical analysis is based on the theory of linear large deformation mechanics, and the rock mass is considered by the monotonous and homogeneous engineering rock mass. Take the typical section in the middle of the tunnel far away from the tunnel entrance to study, and take the 2 m width along the axis of the tunnel, so we can simplify the problem to the plane strain problem without considering the influence of tunneling.

Theoretically, for the circular caverns with larger burying depth, the range of stress redistribution in surrounding rock mass is limited. The range of stress redistribution is generally considered to be only within the

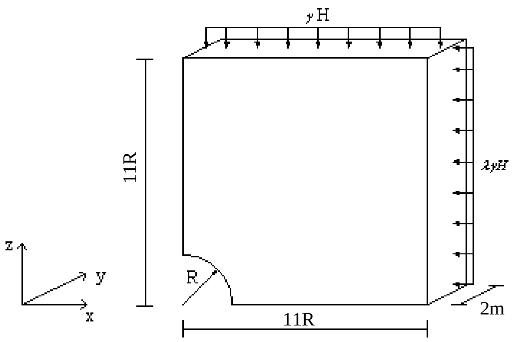

Fig. 1 Computational model

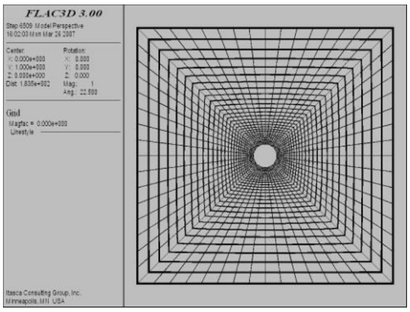

Fig. 2 Mesh generation diagram

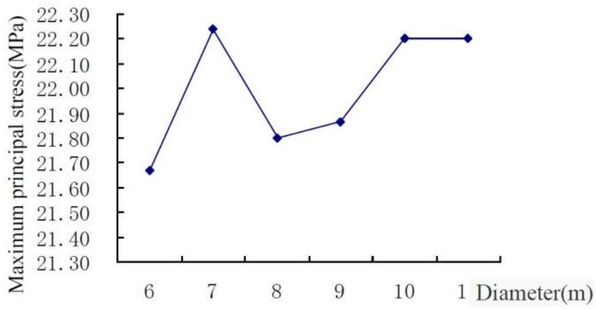

(a) Maximum principal stress value

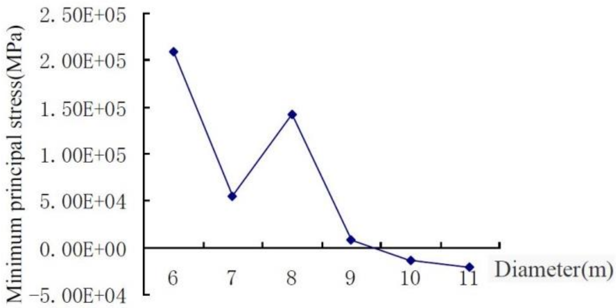

(b) Minimum principal stress value

Fig. 3 Variation curve of principal stress value of tunnel surrounding rock

radius of 3~5 times of the chamber radius.In order to ensure the reliability of the calculation, the numerical analysis area takes about 12 times the diameter of the tunnel, that is,the boundary taken by the numerical analysis area is larger than that of the surrounding rock after the excavation. The Y axis along the direction of the tunnel longitudinal axis, Z axis along the vertical direction, X axis horizontally. In the calculation process, the gradient stress load is applied as the boundary condition between the left and right sides of the model, and the bottom of the model is fixed with the fixed constraint.The initial stress is applied at the top of the model, the size of which is the gravity stress of the overlying rock mass, and the horizontal stress is applied to the left and right side and the front and back boundaries. The boundary conditions of the calculation model, the established coordinate system and the mesh subdivision are shown in Figs. 1 and 2.

The roof of the tunnel is subjected to the pressure of the overlying rock mass, and the weight of the rock and soil is in the form of physical strength in the whole computational domain.The force exerted on the front and left boundary of the tunnel is the horizontal lateral pressure caused by the self gravity of the rock and soil, and the size of the lateral pressure is $\sigma_x=\lambda\sigma_z$ (σ_z is the self gravity stress of the rock and soil, λ is the side pressure coefficient).

4. Calculation results and analysis

4.1 Influence of tunnel diameter on the displacement and stress of surrounding rock and lining

In numerical simulation, the control depth is 500 m, the lateral pressure coefficient λ=1, the inner diameter of the tunnel is 5-10 m, and the lining thickness is 0.5 m. The change rule of displacement, stress and plastic zone of surrounding rock under different excavation diameter is compared.

After tunneling, under the condition of no lining, the maximum principal stress, the minimum principal stress, the maximum radius of the plastic zone in the surrounding rock and the maximum displacement around the surrounding rock vary with the diameter of the tunnel, which are shown in Figs. 3-6.

In Fig. 3, it can be observed that the maximum principal stress generally increases with the increase of the diameter of the tunnel, and because the location of the maximum principal stress is located inside the surrounding rock of the tunnel, the effect of the maximum principal stress on the overall stability of the rock mass is not very large; the minimum principal stress with hole diameter decreases, when the tunnel diameter is close to 10 m, the minimum principal stress is negative, and the minimum principal stress appears in the tunnel, on the stability of surrounding rock is extremely unfavorable, so from the surrounding rock stability considering the hole diameter should not be too large, the best no more than 10 m; generally speaking, the influence of the variation of the hole diameter on the maximum principal stress and the minimum principal stress is not very large. Therefore, the influence of the change of the hole diameter on the two can not be considered in the design. But when the diameter of the hole is large, special attention should be paid to the negative value of the minimum principal stress.

In Fig. 4, it can be observed that the maximum plastic zone radius of the tunnel surrounding rock increases with the increase of the hole diameter. When the diameter of the cavity is 9 m, the plastic zone increases obviously than the

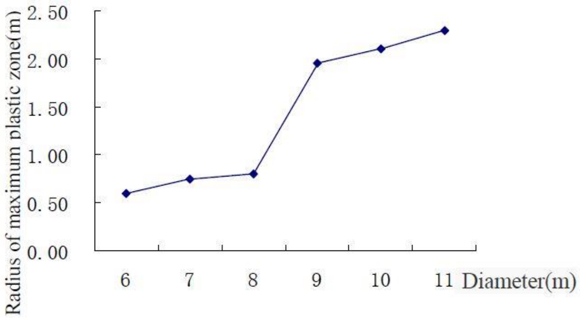

(a) Maximum plastic zone radius

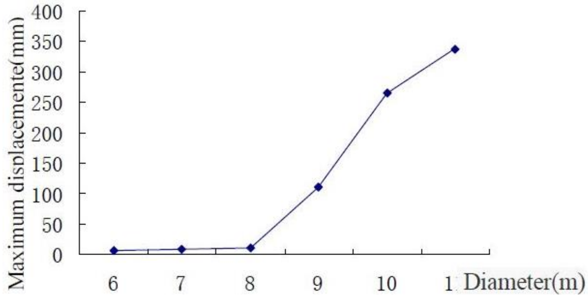

(b) Maximum displacement

Fig. 4 Variation of the plastic zone radius and displacement of tunnel surrounding rock

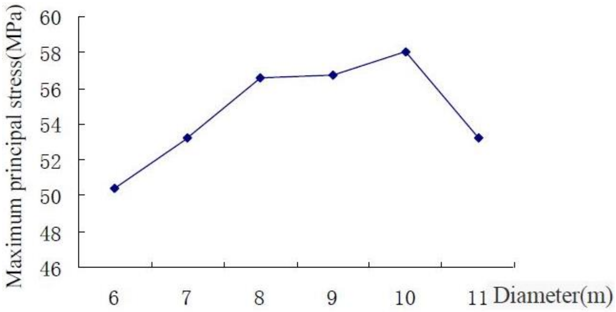

(a) Maximum principal stress value

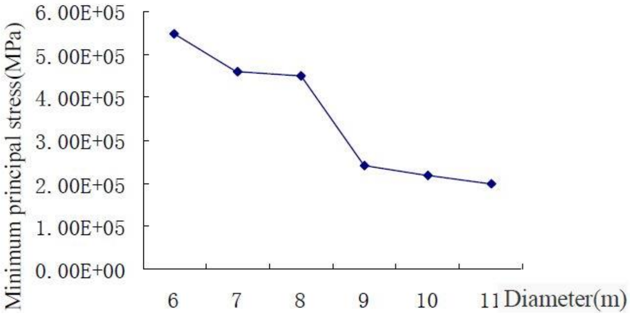

(b) Minimum principal stress value

Fig. 5 Variation curve of principal stress value of lining

hole diameter 8 m, and increases nearly 2 times, and the value is 2 m; with the increase of the hole diameter, the maximum displacement of tunnel surrounding rock increases (the maximum displacement of tunnel surrounding rock have appeared in the top part), both the maximum displacement of X and Z direction are also increased with the increase of the hole diameter,In particular, when the hole diameter reaches 9 m, there is a sharp increase than the hole diameter is 8 m, the tendency

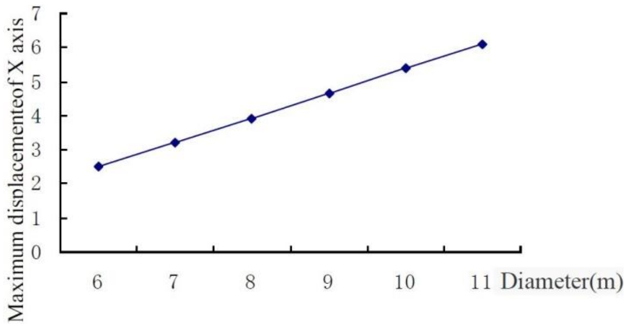

(a) X axis

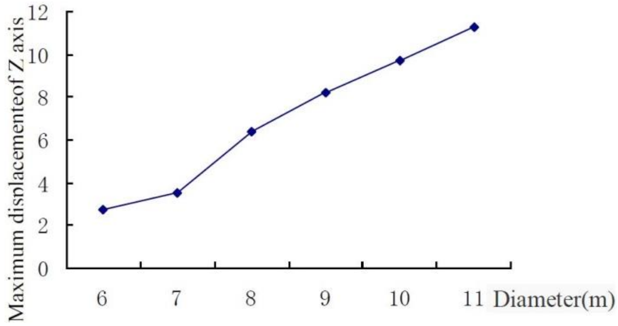

(b) Z axis

Fig. 6 Maximum displacement curve of X and Z axis of lining

of increase after remain unchanged, displacement increases very fast, when the hole diameter reaches 11 m, the maximum displacement of tunnel surrounding rock has reached 400 mm, the maximum displacement around the tunnel from the control point of view, the water conveyance tunnel the hole diameter should be controlled within 8-9 m, in order to achieve the purpose of security and economy.

After the tunnel is excavated and lined, the maximum stress, the minimum principal stress, the horizontal direction and the maximum displacement in the vertical direction vary with the diameter of the tunnel, as shown in Figs. 5-6.

Compared with Fig. 3(a) to Fig. 4(b) and Fig. 5(a) to Fig. 6(b), it can be seen that the maximum principal stress, the minimum principal stress and the maximum displacement around the lining vary with the variation of the hole diameter, which is basically consistent with the law of the variation of the corresponding parameters in the surrounding rock with the variation of the hole diameter.

The maximum displacement of lining in the roof, so in the construction process, should avoid lining the seams in the position.

4.2 Influence of side pressure coefficient on displacement and stress of surrounding rock and lining

The buried depth is 500 m, the diameter of the tunnel is 7 m and the thickness of the lining is 0.5 m as the basis for calculation, the lateral pressure coefficients are 0.5, 1, 1.5, 2 and 2.5, the relationship between lateral pressure coefficient and stress, strain and displacement in surrounding rock and lining is systematically discussed.

The maximum principal stress, the minimum principal

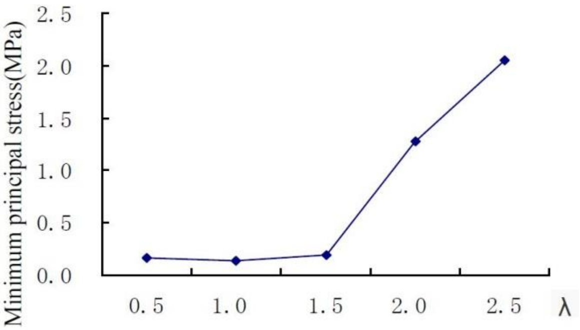

(a) Minimum principal stress value

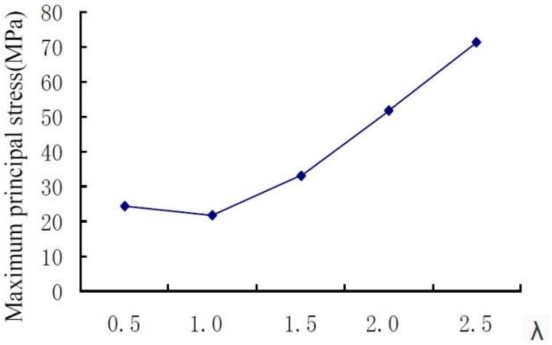

(b) Maximum principal stress value

Fig. 7 The relation curve of principal stress and lateral pressure coefficient

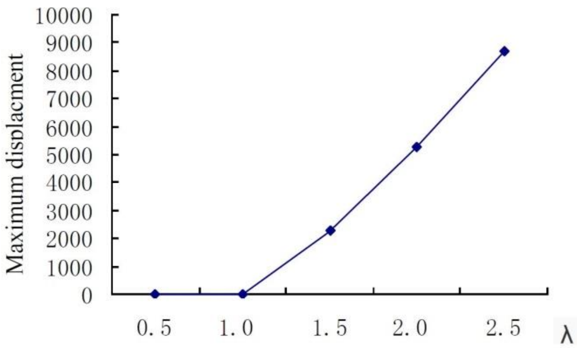

(a) Maximum displacement

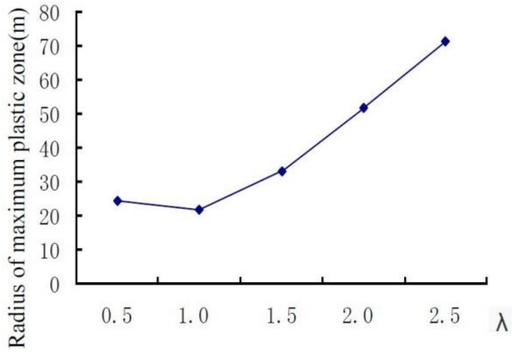

(b) Radius curve of maximum plastic zone

Fig. 8 The curve of the radius and displacement of the plastic zone with the lateral pressure coefficient

stress, the maximum radius of the plastic zone in the surrounding rock and the maximum displacement around the surrounding rock vary with the variation of the lateral pressure coefficient, which is shown in Figs. 7-8.

It can be observed in Fig. 7 that with the increase of lateral pressure coefficient, the minimum principal stress value of tunnel surrounding rock will also increase, and the change is very obvious. The lateral pressure coefficient is less than 1.5, surrounding the maximum tensile stress changes little; while in the lateral pressure coefficient is greater than 1.5, surrounding the maximum tensile stress increases, the lateral pressure coefficient is 2, the tensile stress has reached 1.3 MPa, and the lateral pressure coefficient reaches 2.5, the largest the tensile stress is larger than 2, and the value of nearly 2 times, reaching 2.1 Mpa.

The change of the lateral pressure coefficient on the maximum principal stress of tunnel surrounding rock (the maximum principal stress is negative, compressive stress, in effect, the surrounding rock) showed a trend of non symmetrical, lateral pressure coefficient reaches the minimum value of 21.82 MPa, then showed a significant linear increase trend in 2.5 when you have reached 71.11 MPa, rock mass has great compressive stress, consistent with the results of numerical simulation and theoretical analysis results.

In Fig. 8, it can be observed that when λ<1, the displacement around the tunnel is very small, the minimum is only 9.8 mm when λ=1; the displacement around the tunnel is increased with the increase of the lateral pressure coefficient has risen sharply, at the age of 1.5 has reached over 2.3 m, with the further increase of the lateral pressure coefficient, the calculation procedure has not only displacement convergence, this time as a reference value, indicating that the surrounding rock has been destroyed, the surrounding rock has lost its self stability.

With the increase of the lateral pressure coefficient, consistent with changes of maximum radius of plastic area and the changes of displacement, when λ=1, the minimum radius of the plastic zone, and the radius of plastic zone is increased dramatically, and in more than 1.5 of the time increased a bit slow, but after more than 2 the increase trend has increased, the lateral pressure coefficient is one of the main factors influencing the surrounding rock should stress and around displacement.

After tunnel excavation, the maximum stress and the minimum principal stress in the lining change with the lateral pressure coefficient, as shown in Fig. 9.

With the change of lateral pressure coefficient, the minimum principal stress on the lining is negative when the lateral pressure coefficient is 1, the lining is compressive stress, and no tensile stress appears, which is very favorable for lining. With the increase of lateral pressure coefficient of the minimum principal stress is sharply increased, the lateral pressure coefficient is 2 when there have been 0.2 MPa tensile stress, while the lateral pressure coefficient is 2.5, the tensile stress has reached 0.5 MPa, the stability of the tunnel lining structure is extremely unfavorable.With the change of lateral pressure coefficient, the minimum principal stress on the lining is negative when the lateral pressure coefficient is 1, the lining is compressive stress, and no tensile stress appears, which is very favorable for lining. With the increase of lateral pressure coefficient of the minimum principal stress is sharply increased, the lateral pressure coefficient is 2 when there have been 0.2 MPa tensile stress, while the lateral pressure coefficient is

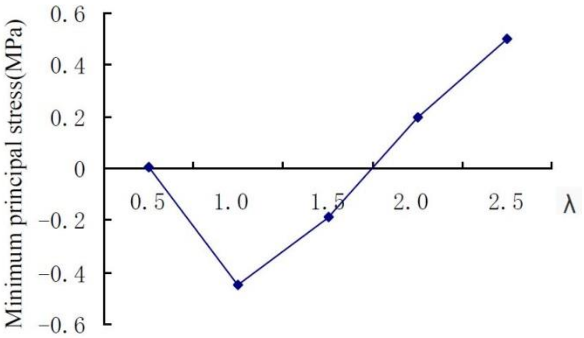

(a) Minimum principal stress

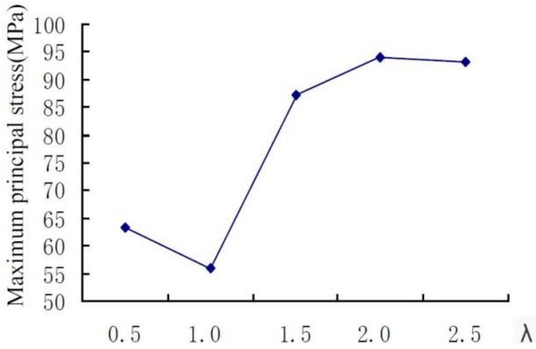

(b) Maximum principal stress

Fig. 9 The relation curve of principal stress and lateral pressure coefficient

2.5, the tensile stress has reached 0.5 MPa, the stability of the tunnel lining structure is extremely unfavorable.

The maximum principal stress on the lining changes in an unsymmetrical relation with the change of the lateral pressure coefficient, hydrostatic pressure in the flat state when the maximum principal stress value is the minimum, then the maximum principal stress increases with the lateral pressure coefficient and presents the obvious growth trend, reached the maximum value at the age of 2 (after there was no increase, this is because the lining has reached the plastic state, the lining has undergone stress damage, the maximum principal stress can be increased).

Fig. 10 is the plastic zone maps of the lining structure at λ=1, 1.5, 2, 2.5, respectively, which can be seen very clearly, when λ=1, the lining structure in the plastic zone, the lining safety; with the increase of lateral pressure coefficient of the lining structure in the plastic zone increases gradually from the lateral pressure coefficient is 1.5 at the top, bottom and side lining for local area began to appear in the plastic zone, to the side the pressure coefficient is 2.5 when lining almost all of the present state of plasticity. It is shown that with the increase of lateral pressure coefficient, the scope of plastic zone appears larger and larger, and the lining state is worse and worse. The most dangerous area of the lining structure can be seen from the plastic zone map of the lining, which is in the region of the shear plastic zone. By comparing and analyzing the range of plastic zone under different lateral pressure coefficients, it can provide theoretical basis for predicting the most dangerous location of lining structure. When using precast segment method to build lining structure, segment joints should try to avoid these positions.

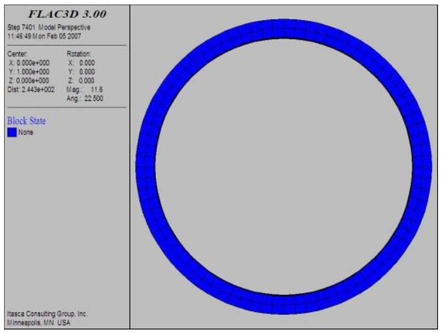

(a) λ=1.0

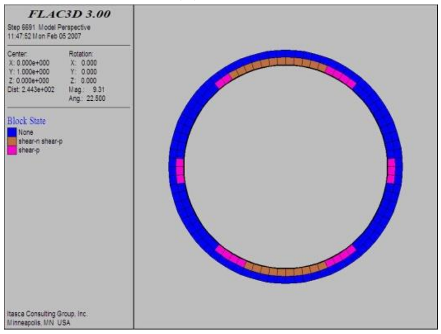

(b) λ=1.5

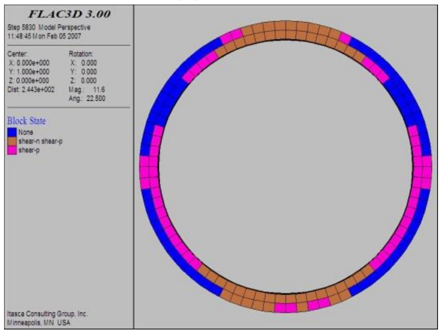

(c) λ=2.0

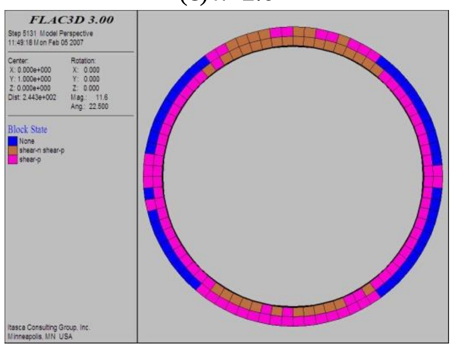

(d) λ=2.5

Fig. 10 Plastic zone map of lining

4.3 Influence of tunnel depth on stress and displacement in surrounding rock and lining structure

The increase of tunnel burial depth directly causes the increase of vertical mountain rock pressure, which will inevitably cause stress and strain and surrounding displacement of tunnel surrounding rock and lining structure. Based on the given conditions: tunnel lining thickness 0.5 m, diameter 3.5 m, and the buried depth changes from 300 m to 1100 m, several typical embedded

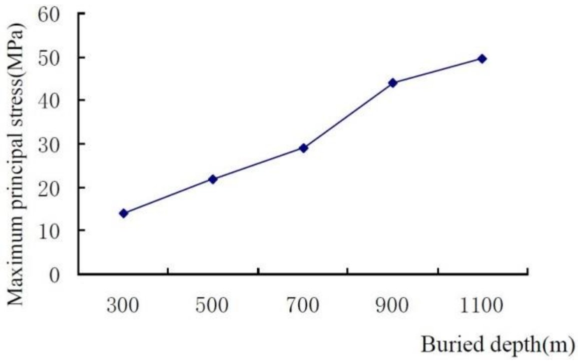

(a) Maximum principal

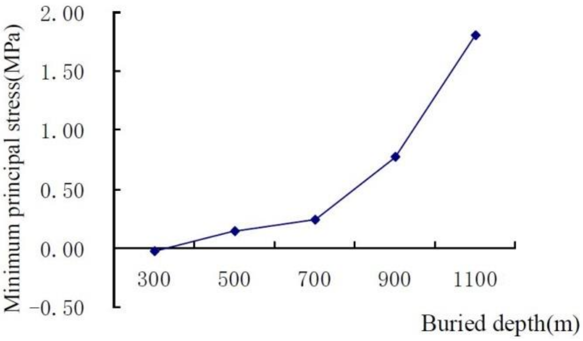

(b) Minimum principal

Fig. 11 The variation curve of principal stress with buried depth

analysis of stress strain and displacement of surrounding rock and lining structure deep in the case, we can fully reach the conclusion that the burial depth in the study of the role and significance.

In Fig. 11, it can be seen as an example, both the stress strain and displacement of tunnel surrounding rock and lining structure, the relationship between theoretical analysis and change with depth and the results are very similar, so the key from the lining structure of the plastic zone varies with the burial depth of the angle of impact analysis the depth of the lining structure and its stability in the engineering design of the role and significance.

Fig. 12 shows the mutual contrast diagram of the plastic zone range in the lining structure when the buried depth of the tunnel is 500 m, 700 m, 900 m and 1100 m. It can be seen that, with the increase of depth, the lining of plastic zone increases, no plastic zone at the time of 500 m lining; buried depth increased to 700 m inner lining plastic zone appeared obvious, while the outer edge is still all in the elastic state; when the depth increased to 900 m, not only inside the plastic outer edge of a further increase in the degree, and also appeared in the local plastic zone; when the depth continues to increase to 1100 m, the lining structure have all appeared plastic state and plastic zone of the shear. Because of the increase of the plastic zone of lining, the displacement of the lining is increased, and then the failure of the whole lining structure is induced. In addition, the position of the shear plastic zone can be seen from the plastic area chart above. The location of this position reminds people to avoid it when arranging the joint.

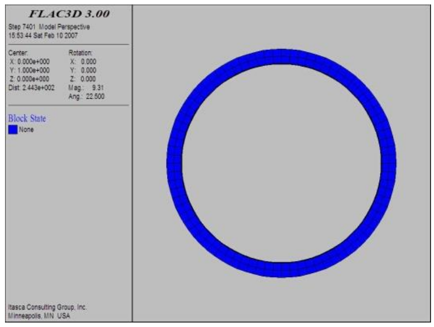

(a) 500 m

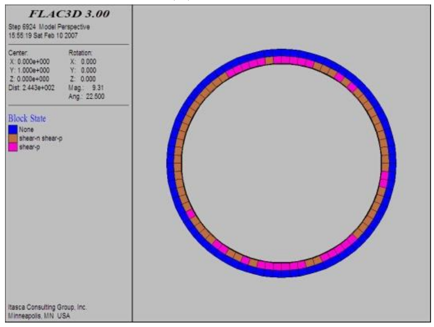

(b) 700 m

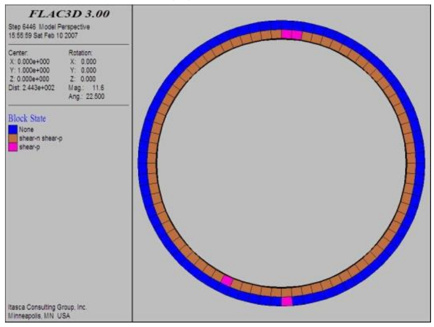

(c) 900 m

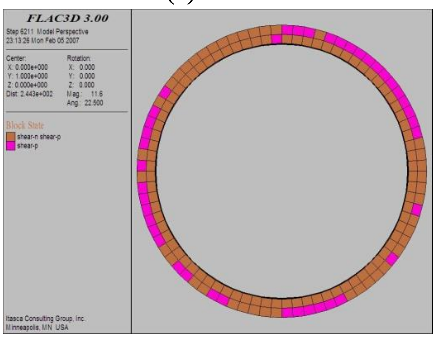

(d) 1100 m

Fig. 12 Plastic zone map of lining with different buried depth

5. Conclusions

The influence of tunnel burial depth, tunnel diameter and lateral pressure coefficient of original rock stress field on the stress and strain of surrounding rock and lining of tunnel is analyzed by FLAC3D numerical simulation software.

- Besides the physical and mechanical parameters of the surrounding rock, the lateral pressure coefficient of the natural stress field, the burying depth of the tunnel and the diameter of the tunnel are the 3 main factors that affect the stress distribution, the radius of the plastic zone of the surrounding rock and the deformation of the lining structure of the surrounding rock and lining structure around the tunnel. The lateral pressure coefficient and the burying depth of tunnel reflect the form and size of natural stress field, which determine the force acting on the deformation of surrounding rock and lining structure, and the diameter of tunnel reflects the disturbance degree of human to the original state of stratum.

• In general, the larger the diameter of the tunnel, the greater the maximum principal stress in the surrounding rock and lining structure, and the smaller the minimum principal stress. However, when the tunnel diameter is large, there will be tensile stress in the surrounding rock. Therefore, considering the radius of the largest plastic zone and the maximum displacement of the surrounding area, the diameter of the water conveyance tunnel should be controlled within a certain range, so as to achieve a safe and economical purpose.

• The size of the side pressure coefficient reflects the uneven degree of stress between various directions in the natural stress field. The natural stress field in the hydrostatic stress state (λ=1), is the most beneficial for the surrounding rock and lining structure; with the natural stress field unbalanced degree increase, the minimum principal stress in surrounding rock and lining are negative (i.e., the tensile stress force), and the maximum principal stress, displacement and plastic zone is sharply increasing trend; natural stress field is not balanced, the maintenance of the tunnel is unfavorable.

• The stress and strain of the tunnel surrounding rock and lining increase with the increase of buried depth, and the plastic zone on the lining also shows an obvious increase trend. With the increase of the plastic zone of the lining, the displacement of the lining increases continuously, which induces the failure of the whole lining structure.

Acknowledgments

This work was supported by Science and Technology Project of Deyang City (No. 2017ZZ066).

References

Ali, A., Saeed S.M. and Zeynab, R. (2018), "Estimation of geomechanical parameters of tunnel route using geostatistical methods", *Geomech. Eng.*, **14**(5), 453-458.

Ardakani, A., Bayat, M. and Javanmard, M. (2014), "Numerical modeling of soil nail walls considering Mohr Coulomb, hardening soil and hardening soil with small-strain stiffness effect models", *Geomech. Eng.*, **6**(4), 391-401.

Chen, Y.J., Zhu, W.S. and Li, S.C. (2016), "New reinforcement algorithms in discontinuous deformation analysis for rock failure", *Geomech. Eng.*, **11**(6), 787-803.

Li, T.C., Lu, Z., Liu, J.Z. and Ma, X.Q. (2014), "Deformation and failure process analysis of rectangular roadway in muddy weakly cemented soft rock strata", *Rock Soil Mech.*, **35**(4), 1077-1084.

Li, Y.H., Lin, Z.B. and Yu, J. (2016), "Experimental study of deformation laws of surrounding rock in deep circular roadway using transparent rock", *J. China Univ. Min. Technol.*, **45**(6), 1104-1110.

Liu, C., Ding, W.Q., Tan, S., Huang, Y.L. and Guo, H.Y. (2016), "Application of the control method for deformation of weak surrounding rock during the construction of tunnel entrance", *Chin. J. Undergr. Sp. Eng.*, **12**, 743-765.

Liu, D. and Chen, X.P. (2015), "Shearing characteristics of slip zone soils and strain localization analysis of a landslide", *Geomech. Eng.*, **68**(1), 33-52.

Liu, D.S. (2015), "Experimental method and analysis of shear strength of rock body", *Chin. J. Undergr. Sp. Eng.*, **11**, 443-446.

Liu, W.R., Peng, C., Li, C.M., Yin, Z.Q., Li, Y. and Zhu, C.Q. (2015), "Stability analysis of surrounding rock of deep underground tunnel", *China Saf. Sci. J.*, **25**(5), 120-125.

Ma, R., Li, G.C., Zhang, N. and Liu, C. (2015), "Analysis on mechanism and key factors of surrounding rock instability in deeply inclined roadway affected by argillation and water seepage", *Int. J. Min. Sci. Technol.*, **25**(3), 465-471.

Małkowski, P. (2015), "The impact of the physical model selection and rock mass stratification on the results of numerical calculations of the state of rock mass deformation around the roadways", *Tunnel. Undergr. Sp. Technol.*, **50**, 365-375.

Nikadat, N. and Marji, M.F. (2016), "Analysis of stress distribution around tunnels by hybridized FSM and DDM considering the influences of joints parameters", *Geomech. Eng.*, **11**(2), 269-288.

Sheng, Q.Y., Miao, C. and Hong, W.J. (2017), "A case study on large deformation failure mechanism of deep soft rock roadway in Xin'An coal mine, China", *Eng. Geol.*, **217**, 89-101.

Siddiquee, M.S.A., Islam, M.S. and Tatsuoka, F. (2013), "Development of a nonlinear model for soft rock and its applications", *Geotech. Geol. Eng.*, **31**(2), 627-45.

Su, D.Z. and Luo, J.J. (2016), "Experimental study and prediction on large section tunnel construction deformation of surrounding rock in soft ground", *Chin. J. Rock Mech. Eng.*, **35**, 4029-4038.

Wang, J.J., Steven, N.W. and Xiao, L.L. (2015), "Numerical simulation of the December 4, 2007 landslide-generated tsunami in Chehalis Lake, Canada", *Geophys. J. Int.*, **201**(1), 372-376.

Xie, H.P., Peng, R.D. and Ju, Y. (2004), "Energy dissipation of rock deformation and fracture", *Chin. J. Rock Mech. Eng.*, **23**(21), 3565-3570.

Yoo, C. (2016), "Effect of spatial characteristics of a weak zone on tunnel deformation behavior", *Geomech. Eng.*, **11**(1), 41-58.

Yu, Y.X., Chen, B.P., Zhang, T. and Zhang, J. (2017), "Back analysis on deformation and failure zone distribution laws of surrounding rock in deep-buried soft rock tunnel", *J. Railw. Eng. Soc.*, **34**(3), 46-52.

Zhu, H.H., Ye, B., Cai, Y.C. and Zhang, F. (2013), "An elasto-viscoplastic model for soft rock around tunnels considering overconsolidation and structure effects", *Comput. Geotech.*, **50**, 6-16.

CC